

Influence of ultrathin water layer on the van der Waals/Casimir force between gold surfaces

G. Palasantzas,¹ V. B. Svetovoy,² and P. J. van Zwol¹

¹*Materials Innovation Institute M2i and Zernike Institute for Advanced Materials, University of Groningen, Nijenborgh 4, 9747 AG Groningen, The Netherlands*

²*MESA+ Institute for Nanotechnology, University of Twente, P.O. Box 217, 7500 AE Enschede, The Netherlands*
(Received 13 February 2009; revised manuscript received 16 April 2009; published 25 June 2009)

In this paper we investigate the influence of ultrathin water layer ($\sim 1\text{--}1.5$ nm) on the van der Waals/Casimir force between gold surfaces. Adsorbed water is inevitably present on gold surfaces at ambient conditions as jump-up-to contact during adhesion experiments demonstrate. Calculations based on the Lifshitz theory give very good agreement with the experiment in the absence of any water layer for surface separations $d \geq 10$ nm. However, a layer of thickness $h \leq 1.5$ nm is allowed by the error margin in force measurements. At shorter separations, $d \leq 10$ nm, the water layer can have a strong influence as calculations show for flat surfaces. Nonetheless, in reality the influence of surface roughness must also be considered, and it can overshadow any water layer influence at separations comparable to the total sphere-plate rms roughness $w_{\text{shp}} + w$.

DOI: 10.1103/PhysRevB.79.235434

PACS number(s): 78.68.+m, 03.70.+k, 85.85.+j, 12.20.Fv

I. INTRODUCTION

When material objects such as electrodes in micro/nanoelectromechanical system are separated by distances of 100 nm or less forces of quantum origin become operative.^{1–3} These are the van der Waals (vdW) and Casimir forces originating from the same physical basis, but having different names due to historical reasons. The van der Waals force is the short-distances asymptotic of this general force, for which one can neglect the retardation of electromagnetic fields, but the Casimir force is realized at larger distances where the retardation is important. The common origin of the forces is nicely explained by the Lifshitz theory,⁴ which is able to describe the transition between the two regimes. It predicts transition between the Casimir and van der Waals forces at separations $d \sim \lambda_p/10$, where $\lambda_p = 2\pi c/\omega_p$ is the plasma wavelength and ω_p is the plasma frequency.^{5,6} Keeping in mind the common origin of the forces, in what follows we will also use a generalized name *dispersive forces*.

At separations below 100 nm the Casimir force is very strong and becomes comparable to electrostatic forces corresponding to voltages in the range 0.1–1 V,^{1–3} while for separations below 10 nm the van der Waals force dominates any attraction.^{7–9} These properties make the dispersive force an important player in nanosciences. Moreover, from the fundamental point of view, measurements of the forces from nano to microscales have attracted strong interest in a search of hypothetical fields beyond the standard model.¹⁰

In the experiments the dispersive forces are usually measured between a sphere and a plate. In the vdW regime the force depends on distance d as $A_H R/6d^2$, where R is the radius of the sphere. Fits of the experimental data yielded an effective Hamaker constant $A_H \approx (7\text{--}25) \times 10^{-20}$ J for gold-water-gold systems.¹¹ On the other hand, for Au-air-Au surfaces studies by Tonck *et al.*¹¹ using the surface force apparatus in the plane-sphere geometry with millimeter size spheres yielded an effective Hamaker constant of $A_H \approx 28 \times 10^{-20}$ J for separations $d > 8.5$ nm. Similar values $A_H \approx 29 \times 10^{-20}$ J (Ref. 12) were obtained from force measurements with atomic force microscope (AFM) at separations

between 12 nm–17 nm. We are using here the term “effective Hamaker constant” because in this distance range the van der Waals asymptotic regime is not fully reached. Fitting the curve force vs distance following from the Lifshitz theory in the range $d = 1\text{--}5$ nm one would find the Hamaker constant to be $A_H \approx 40 \times 10^{-20}$ J as it is expected between metal surfaces.¹³ However, in this distance range the experimental determination of the constant for Au-air-Au is problematic due to the strong influence of surface roughness and the strong jump-up-to-contact by formation of capillary bridges due to adsorbed water.¹⁴ It was found that even for the lowest attainable relative humidity $\sim 2\% \pm 1\%$, large capillary forces are still present.

In this paper we use the term adsorption in sense of physisorption when the electronic structure of atoms or molecules is barely perturbed upon adsorption. Formation of capillary bridges takes place due to water adsorbed on Au. We can expect that the surface of Au is covered with an ultrathin water layer, which is present on almost all surfaces exposed to air. Experiment¹⁴ suggests that the thickness of this layer is in the nanometer range. The natural questions one could ask is how thick the water layer is, and what is the influence of this layers on the dispersive force? At short separations, $d \leq 20$ nm, these questions become of crucial importance because they place doubts on our understanding of the dispersive forces when experiments under ambient conditions are compared with predictions of the Lifshitz theory. In this paper we are performing the first steps to answer these questions comparing experimental data at short separations with the theoretical predictions for Au covered with a thin layer of water. The problem is rather nontrivial since surface wettability can be influenced by other adsorbates (e.g., hydrocarbons leading to incomplete wetting), the optical properties of real films must be measured correctly,¹⁵ as well as the influence of surface roughness has to be taken into account.^{9,16} The latter lead to uncertainties in the separation distance of real surfaces, and its contribution to the force has to be carefully scrutinized.^{16,17}

The paper is organized as follows. In Sec. II we provide information on surface roughnesses and force measurements in the AFM experiment, and discuss the distance upon the

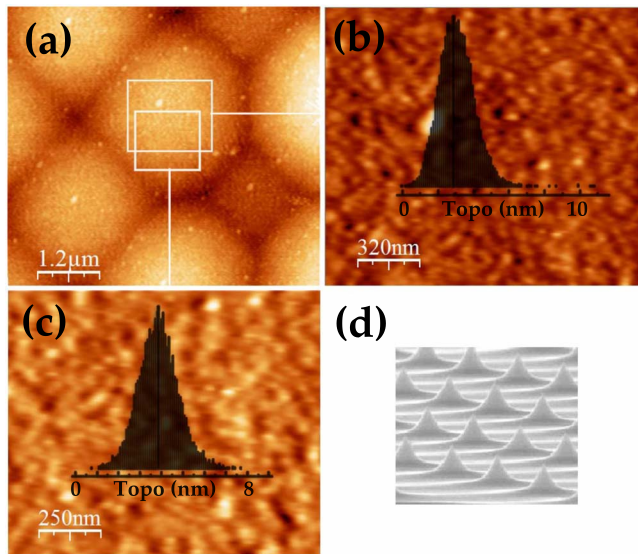


FIG. 1. (Color online) (a) Reverse AFM scan of a sphere that has been used for measurement. (b) Surface scan and height distribution with large spots. (c) Surface scan and height distribution without large spots. The full width of the roughness distribution of the sphere without the spots in (c) is about 6 nm. (d) Grid used for the inverse AFM scans of the contact area.

contact deduced from the measured roughness. In Sec. III A the main definitions of the Lifshitz theory are given, and the roughness correction is related with the measured roughness profile. The dielectric function of water at the imaginary frequencies is described in Sec. III B. In Sec. III C we discuss optical data for gold in relation to the adsorbed water, and in Sec. III D the results of the dispersive force calculations are given for nonzero adsorbed water layer. Our conclusions are presented in Sec. IV.

II. EXPERIMENTAL

The dispersive force is measured using the picoforce AFM,¹⁸ between a sphere with a diameter of 100 μm attached on a 240 μm long cantilever of stiffness $k=4$ N/m (as given by the manufacture), and an Au coated silicon plate. Both sphere and plate are coated with 100 nm of Au, and afterwards their root-mean-square (rms) roughness was measured by AFM (see Figs. 1 and 2). Analysis of the area on the sphere where the contact with the substrate occurs was performed by inverse imaging (Fig. 1).^{12,17} The histograms in Figs. 1 and 2 show the number of pixels corresponding to a given height.

Notably the sphere roughness of 1.8 ± 0.2 nm rms¹⁶ is an average over a large area where relatively high spots are observed [see Figs. 1(a) and 1(b)], which increase the rms roughness value. For plates surfaces (Fig. 2) these spots were absent leading to the rms roughness 1.3 ± 0.2 nm.¹⁶ Although the high spots within the contact area may increase the contact separation between bodies, d_0 , they deform fast when pushing surfaces into contact to determine the deflection sensitivity. This is demonstrated by inverse imaging (see Ref. 14 for detailed explanations) and mechanics calcula-

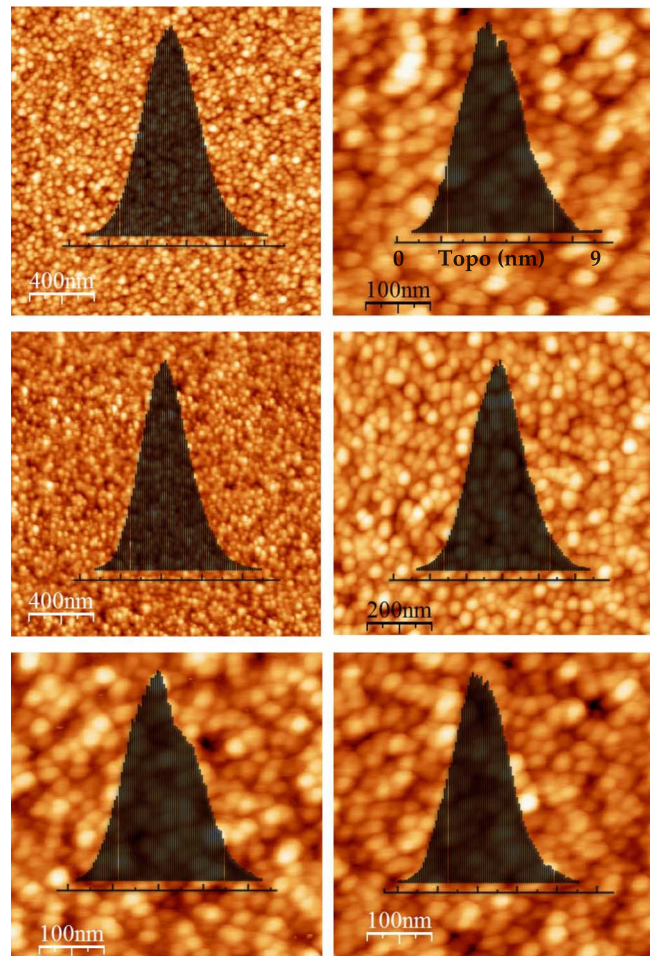


FIG. 2. (Color online) Scan areas and height distributions of the Au films deposited on Si substrate used for the force measurements.

tions also confirm it.¹⁹ Locally without the spots or with the deformed spots the roughness obtained by inverse imaging was 0.8–1.2 nm rms or $w_{\text{sph}}=1 \pm 0.2$ nm within the contact area of size 1 μm [Fig. 1(c)].

Stiff cantilevers used in this experiment do not allow low-voltage electrostatic calibration (<0.5 V) at small separations. To obtain the contact separation due to roughness d_0 we used a different procedure. One can define the distance between rough bodies as the distance between zero roughness levels. From the histograms in Figs. 1 and 2 it is clear that the zero roughness level corresponds to the maximum of the distribution. Without the spots mentioned above these distributions are approximately symmetric. Two rough surfaces in contact are separated by the distance d_0 , which is half of the distance between lowest and highest points of the rough profile (full width of the histogram) for the sphere plus the same for the plate. In this way we found $d_0 = 7.5 \pm 1$ nm from multiple AFM scans at different locations.

It has to be stressed that this direct way (from the definition) to determine d_0 is in good correspondence with what we would expect from the electrostatic calibration. In Refs. 9 and 16 the relation $d_0 \approx (3.7 \pm 0.3) \times (w + w_{\text{sph}})$ was found from the electrostatic calibration. In our case the total rms roughness (sphere and plate) is $w + w_{\text{sph}} = 1.3 + 1 = 2.3$ nm.

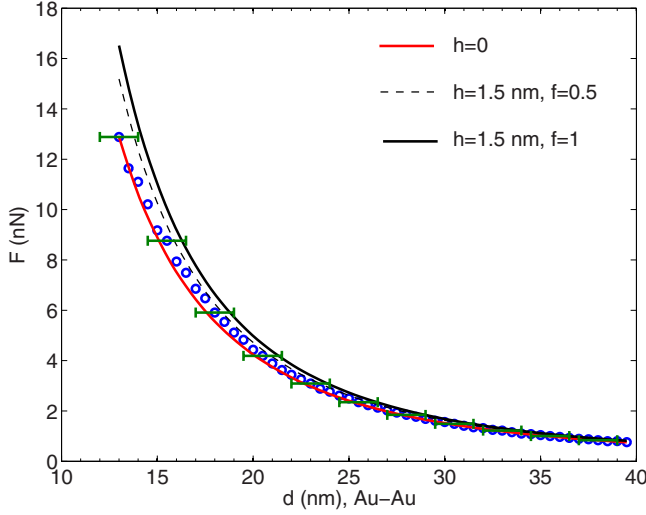


FIG. 3. (Color online) Experimental data for the force vs distance (circles) and theoretical prediction without water layer (red curve). Errors in the absolute separation are shown for some points by the bars. The continuous black curve is the prediction for 1.5 nm continuous water layer. The dashed black curve corresponds to the same water layer with 50% of voids.

Using this relation we can find d_0 within one standard deviation from that found above from the first principle definition.

The calibration of the deflection sensitivity, cantilever stiffness k , and contact potential V_0 was done in the same way as in previous work.⁹ Electrostatic fitting in the range of distances 1–4 μm and voltage interval $\pm(3\text{--}4.5)$ V yielded the cantilever stiffness $k=8.55 \pm 0.38$ N/m (with the sphere attached) and contact potential $V_0=10 \pm 10$ mV. After calibration, the dispersive force was measured and averaged (using 40 force curves at 20 different locations yielding an average of 800 curves). The result is shown in Fig. 3 together with the theoretical curves (see Sec. III) without (red) or with (black) adsorbed water layer. Each experimental point (circles) is defined with rather large uncertainty in distance, which is shown by the horizontal bars for some points. Indeed, the main uncertainty ΔF in the dispersive force at short distances comes from the uncertainty $\Delta d=1$ nm in the separation upon contact $d_0=7.5 \pm 1$ nm. The error in the force due to error in d_0 can be estimated as $(\Delta F/F) \approx c(\Delta d_0/d_0)$, where $c \approx 2.5$ in the investigated range of distances. Other sources of errors include the error of the cantilever spring constant $\Delta k/k \approx 4\%$ and the error in the radius of the sphere $\Delta R/R=2\%$. These errors propagated to the force are negligible in comparison with that arising from $\Delta d_0/d_0$. Finally, at separations $d > 100$ nm the force is rather weak, and the error is dominated by thermomechanical noise as it was explained in former studies.¹⁶

Evaluation of the force based on the Lifshitz theory requires the use of the optical properties of the interacting materials as input data. The optical properties of gold films were measured in air with ellipsometry in the wavelength range 137 nm–33 μm .¹⁵ Outside of this interval at low frequencies ($\lambda > 33$ μm) the data were extrapolated according to the Drude model with the plasma frequency $\omega_p = 7.84 \pm 0.07$ eV and the relaxation frequency γ

$= 49.0 \pm 2.1$ meV. The Drude parameters were determined from the measured part of the dielectric function.¹⁵ At high frequencies ($\lambda < 137$ nm) the method of extrapolation did not play any role, and the data were taken from the handbook.²⁰

III. THEORY

A. Gold-gold interaction in the Lifshitz theory

First we are going to calculate the interaction energy between two plates E_{pp}^{flat} . To be more precise it must be the free energy if we consider the interaction at finite temperature T . Here, however, we will neglect the thermal effect because our intention is to calculate the force in the short-distance range $d < 100$ nm. It is known that for these separations and at room temperature the thermal correction is small.²¹ Physically it means that the zero-point quantum fluctuations of the electromagnetic field give the main contribution to the interaction, while thermally excited fields can be neglected. In this case instead of summation over the discrete set of Matsubara frequencies, one can integrate over a continuous imaginary frequency.⁴ The resulting interaction energy corresponding to zero temperature can be presented in the following form:

$$E_{pp}^{\text{flat}}(d) = \frac{\hbar}{2\pi} \sum_{\mu} \int_0^{\infty} d\xi \int \frac{d^2q}{(2\pi)^2} \ln(1 - R_{\mu} e^{-2dk_0}). \quad (1)$$

Here the index $\mu=s,p$ is running two possible polarization states of the electromagnetic field, and R_{μ} is the product of the Fresnel reflection coefficients for plates 1 and 2: $R_{\mu} = r_{1\mu} r_{2\mu}$. The integration variables have the physical meaning of the imaginary frequency ξ , and the wave vector $q=|\mathbf{q}|$ along the plates.

Here it will be assumed that both interacting surfaces are the same: $r_{1\mu}=r_{2\mu}=r_{\mu}$. For what follows it will be convenient to use index 2 for quantities related to gold. If no additional layer on the gold surface exists, then the Fresnel coefficients can be written as

$$r_s = \frac{k_0 - k_2}{k_0 + k_2}, \quad r_p = \frac{\varepsilon_2 k_0 - k_2}{\varepsilon_2 k_0 + k_2}, \quad (2)$$

where k_0 and k_2 are defined as the normal components of the wave vector in vacuum and in Au, respectively. These components are

$$k_0 = \sqrt{\xi^2/c^2 + q^2}, \quad k_2 = \sqrt{\varepsilon_2 \xi^2/c^2 + q^2}. \quad (3)$$

In Eqs. (1)–(3) the dielectric function of gold ε_2 has to be understood as the function at imaginary frequencies: $\varepsilon_2 = \varepsilon_2(i\xi)$. This function cannot be directly measured, but it can be expressed with the Kramers-Kronig relation via the observable dielectric function $\varepsilon_2(\omega)$ at real frequencies ω

$$\varepsilon_2(i\xi) = 1 + \frac{2}{\pi} \int_0^{\infty} d\omega \frac{\omega \varepsilon_2''(\omega)}{\omega^2 + \xi^2}. \quad (4)$$

Note that only the imaginary part of the dielectric function $\varepsilon_2''(\omega)$ contributes to $\varepsilon_2(i\xi)$. The fact that the dispersive force

depends on $\varepsilon_2(i\zeta)$ makes the material dependence of the force sometimes confusing. For example, thin metallic film transparent for visible light gives very significant contribution to the force.²² On the other hand, a hydrogen-switchable mirror that changes from reflection to transmission in visible light does not give a measurable effect.²³

For practical evaluation of the interaction energy it is convenient to change variables in Eq. (1). Namely, instead of q one can introduce $x=2dk_0$. With this variable the integral will run from $\xi=\zeta/\omega_c$ to ∞ , where

$$\omega_c = \frac{c}{2d} \quad (5)$$

is the characteristic imaginary frequency (it is not a characteristic frequency in real domain). Because of exponent in the integrand the integral over x converges fast. However the integral over ζ running from 0 to ∞ is not convenient for numerical evaluation. This problem can be solved by substituting $\zeta=xt\omega_c$. Now t will run from 0 to 1, and in terms of x and t numerical calculation of the integral in Eq. (1) becomes convenient:

$$E_{pp}^{\text{flat}}(d) = \frac{\hbar c}{32\pi^2 d^3} \sum_{\mu} \int_0^1 dt \int_0^{\infty} dx x^2 \ln(1 - R_{\mu} e^{-x}). \quad (6)$$

The roughness correction can be calculated as follows. The force between a sphere and a plate F_{sp} is related with the interaction energy per unit area between two plates E_{pp} by the relation:

$$F_{sp}(d) = 2\pi R E_{pp}(d), \quad (7)$$

where d is the minimal distance between bodies and R is the sphere radius. Relation (7) holds true in the limit $R \gg d$ that is the case for our experiment. Roughness gives contribution to the energy E_{pp} , which can be presented as

$$E_{pp} = E_{pp}^{\text{flat}} + \delta E_{pp}^{\text{rough}}, \quad (8)$$

where the first term corresponds to the interaction energy between plates.

The second term in Eq. (8) is responsible for the roughness correction. It can be presented in the form²⁴

$$\delta E_{pp}^{\text{rough}} = \int \frac{d^2 k}{(2\pi)^2} G(k, d) \sigma(k). \quad (9)$$

Here $\sigma(k)$ is the roughness spectrum and $G(k, d)$ is the response function derived in²⁴ both are functions of the wave number k . For self-affine roughness $\sigma(k)$ scales as²⁵ $\sigma(k) \propto k^{-2-2H}$ for $k\xi \gg 1$ and $\sigma(k) \propto \text{const}$ for $k\xi \ll 1$. The parameters ξ and H are the correlation length and roughness exponent, respectively. For the roughness calculations we used the roughness model in Fourier space.²⁶

$$\sigma(k) = \frac{AHw^2\xi^2}{(1+k^2\xi^2)^2}, \quad A = \frac{2}{[1 - (1+k_c^2\xi^2)^{-H}]}, \quad (10)$$

where w is the rms roughness, and $k_c \sim 1 \text{ nm}^{-1}$ is a lower roughness cutoff.

For actual calculations we took for the roughness parameters in $\sigma(k)$ the values: $w_{\text{sph}}=1.0 \text{ nm}$, $w=1.3 \text{ nm}$, lateral

correlation lengths $\xi=20 \text{ nm}$, and roughness exponent $H=0.9$.¹⁶ At separations $d > 10 \text{ nm}$ roughness can still play significant role by increasing the force. It has to be noted that relation (9) derived within the scattering theory²⁴ is applicable for $d \gg w + w_{\text{sph}}$ and small local surface slopes. For smaller d a much stronger roughness effect is expected increasing the force up to five times or more with respect to that of flat surfaces as former studies indicated.⁹

We performed calculations of the force between a sphere of radius $R=50 \mu\text{m}$, and a plate without any water layers using Eqs. (6)–(10). As the dielectric function of Au film we used the data for sample 3 from Ref. 22. The results are presented in Fig. 3 by the red line. One can see that the force without any water layer agrees reasonably well with the experimental data. The question is what restriction can be derived from this agreement on the thickness of the water layer on the gold surface?

B. Dielectric function of water

In order to understand how the water layer will contribute to the force, we have to know first the dielectric function of water at imaginary frequencies $\varepsilon_1(i\zeta)$. Water is a well-investigated medium, and there are a few works where the dielectric function was calculated. Parsegian and Weiss²⁷ fitted $\varepsilon_1(\omega)$ by a number of Lorentzian oscillators as it is traditionally used by spectroscopists. Then the function $\varepsilon_1(i\zeta)$ can be found by analytic continuation. This method, however, does not always give sufficient precision. For example, refitting of the same input data used in²⁷ gave considerably different result.²⁸ Recently a new analytical model for the dielectric function was proposed.²⁹

A more reliable approach can be based on the direct use of the optical data of water. It was realized in Ref. 30 where $\varepsilon_1(i\zeta)$ was found from available optical data in a wide range of frequencies. The authors were directed to calculation of the van der Waals force at rather small separations $d \sim 1 \text{ nm}$. The important imaginary frequencies where $\varepsilon_1(i\zeta)$ has to be known with the best possible precision are around $\zeta \sim \omega_c = c/2d$. For $d \sim 1 \text{ nm}$ important frequencies are $\zeta \sim 100 \text{ eV}$. To have $\varepsilon_1(i\zeta)$ in this frequency range one has to integrate in the dispersion relation (4) (but for ε_1) at $\omega \geq 100 \text{ eV}$. For these high frequencies the directly measured quantity is $\text{Im}[1/\varepsilon(\omega)]$. The real part of $1/\varepsilon(\omega)$ must be restored with the Kramers-Kronig relation. The complete procedure for calculation of $\varepsilon(i\zeta)$ is rather complex.³⁰ In our case, for $d \geq 10 \text{ nm}$ this procedure can be significantly simplified.

Segelstein³¹ compiled the data for the absorption coefficient of water in very wide range of wavelengths from 10 nm to 1 m. These data can be used instead of $\varepsilon_1''(\omega)$ to calculate $\varepsilon_1(i\zeta)$. The absorption coefficient $\mu(\omega)$ is related with the imaginary part of the complex refractive index $\tilde{n}(\omega) = n(\omega) + ik(\omega)$ by the relation $\mu(\omega) = 2\omega k(\omega)/c$. Between $n(\omega)$ and $k(\omega)$ exists similar dispersion relation as between $\varepsilon_1'(\omega)$ and $\varepsilon_1''(\omega)$:

$$\tilde{n}(i\zeta) = 1 + \frac{2}{\pi} \int_0^{\infty} d\omega \frac{\omega k(\omega)}{\omega^2 + \zeta^2}. \quad (11)$$

If we know $\tilde{n}(i\zeta)$ then $\varepsilon_1(i\zeta)$ can be expressed as $\varepsilon_1(i\zeta) = \tilde{n}^2(i\zeta)$. This is true because both functions \tilde{n} and ε_1 are analytical.

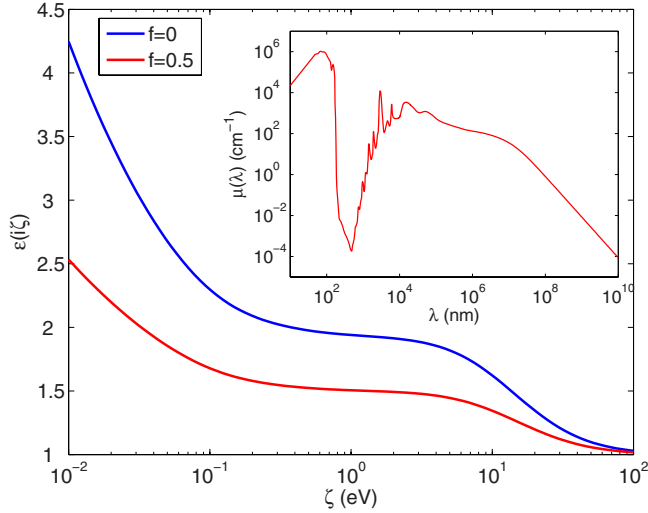


FIG. 4. (Color online) The dielectric function of water at imaginary frequencies. The blue curve is for bulk water (no free volume, $f=0$). The red curve corresponds to water with 50% of free volume, $f=0.5$ (see Sec. III D). The inset shows the compiled data for absorption coefficient used as input data to calculate $\varepsilon_1(i\zeta)$.

The resulting dielectric function of water calculated at the imaginary frequencies is presented in Fig. 4. The inset shows the compiled data³¹ for the absorption coefficient of water $\mu(\lambda)$. Our result is close to that in Ref. 30 and deviates from both in²⁷ and²⁸. It is interesting to note that $\varepsilon_1(i\zeta)$ is still far from its static value $\varepsilon_1(0) \approx 80$ even at $\zeta = 0.01$ eV. The static value is reached only at $\zeta \sim 10^{-6}$ eV. This is a specific property of water.

C. Water film and optical data

The optical properties of our gold films were measured at ambient conditions.¹⁵ An ultrathin film of water is already incorporated in the optical response of these films. It means that the force calculated with the dielectric function of nominal gold could already include some effect of water. Then the agreement between forces measured and predicted theoretically for pure gold becomes questionable. Therefore, the first question to answer is how well we may know the dielectric function of gold samples from measurements in ambient conditions? This question has also an independent interest for the community dealing with the Casimir effect. Moreover, one could try to extract information on thickness of water films from optical measurements. These problems are closely related and we will analyze them in this subsection.

The ellipsometry can give the “pseudodielectric” function of the investigated material as

$$\langle \varepsilon \rangle = \sin^2 \vartheta \left[1 + \tan^2 \vartheta \left(\frac{1 - \rho}{1 + \rho} \right)^2 \right], \quad (12)$$

where ϑ is the angle of incidence, and ρ is the directly measured complex ratio of the reflection coefficients $\rho = r_p/r_s$. If the investigated material is a pure gold film, then $\langle \varepsilon \rangle$ as calculated from Eq. (12) will correspond to the dielectric function of Au and the reflection coefficients $r_{s,p}$ will coincide with that in Eq. (2).

If there is a water layer of thickness h on top of gold film, then the reflection coefficients entering in Eq. (12) will be different. Let us enumerate the media air-water-gold by increasing indexes 0-1-2. Then for both polarizations we have

$$r = \frac{r_{01} - r_{21} e^{2ik_1 h}}{1 - r_{01} r_{21} e^{2ik_1 h}}, \quad (13)$$

where the reflection coefficients r_{ij} on the border between media i and j are defined as

$$r_{s,ij} = \frac{k_i - k_j}{k_i + k_j}, \quad r_{p,ij} = \frac{\varepsilon_j k_i - \varepsilon_i k_j}{\varepsilon_j k_i + \varepsilon_i k_j}. \quad (14)$$

Since we expect that the thickness of the water layer is small (~ 1 nm) then the phase factor $k_1 h$ will be small $|k_1 h| \ll 1$ at all frequencies covered by the ellipsometers. This is true because in the investigated frequency range $|\varepsilon_1(\omega)| \lesssim 2$. For this reason the measured pseudodielectric function $\langle \varepsilon \rangle$ only slightly deviates from the dielectric function of gold ε_2 :

$$\langle \varepsilon \rangle = \varepsilon_2 + \delta\varepsilon, \quad \left| \frac{\delta\varepsilon}{\varepsilon_2} \right| \ll 1. \quad (15)$$

Using the perturbation theory in $\delta\varepsilon$ one can find from Eqs. (12)–(14) the expression for the relative correction to the dielectric function of Au:

$$\frac{\delta\varepsilon}{\varepsilon_2} = i \frac{4\pi h}{\lambda} \sqrt{\langle \varepsilon \rangle - \sin^2 \vartheta} \frac{\langle \varepsilon \rangle - \varepsilon_1}{\langle \varepsilon \rangle - 1} \cdot \frac{\varepsilon_1 - 1}{\varepsilon_1}. \quad (16)$$

This equation precisely coincides with that presented by Aspnnes in Ref. 32.

If the dielectric functions of gold ε_2 and water ε_1 are known, then using Eqs. (15) and (16) one could find the film thickness h . This can be performed by the best fit of the known ε_2 with the calculated $\langle \varepsilon \rangle - \delta\varepsilon$. However, as it was demonstrated¹⁵ the optical properties of opaque Au films depend on the preparation method on the level, which cannot be ignored. For this reason ε_2 is essentially unknown.

The relative correction (16) is not negligible at low and high frequencies. At low frequencies the ratio h/λ is small but $\langle \varepsilon \rangle$ is large as it is the case for all good conducting materials. At the largest investigated wavelength $\lambda = 30$ μm and $h = 1$ nm, the correction is about 3%. However, for $\lambda > 20$ μm the noise in the data becomes significant, and this correction is below the noise level. If h is larger, we could in principle determine its value. This is because at low frequencies ε_2 can be described by the Drude model, and we can determine h together with the Drude parameters ω_p and γ . This procedure was applied for all investigated Au films but minimization gave unreasonable values of the parameters including a negative water layer thickness. Moreover, the target function used in the minimization is larger than that in the case $h=0$. This probably means that h is small enough so that the correction $\delta\varepsilon$ is on the noise level.

In the high-frequency limit the correction is defined by the ratio h/λ , which is not very small. This frequency range corresponds to the interband absorption of gold where the dielectric function ε_2 cannot be predicted. For this reason we cannot determine h because we have no reliable value to compare with $\langle \varepsilon \rangle - \delta\varepsilon$.

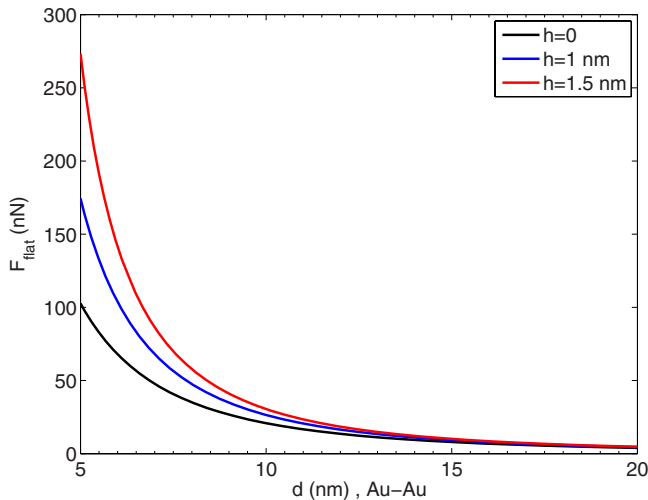


FIG. 5. (Color online) The force between a flat sphere ($R = 50 \mu\text{m}$) and a plate in the range of small separations between gold surfaces. The curves correspond to different thicknesses h of the water layer.

We can conclude that the dielectric function measured ellipsometrically is a good approximation for the dielectric function of pure gold even if there is a layer of adsorbed water. Information on the thickness of the water layer $h \sim 1 \text{ nm}$ cannot be extracted from the data since it is below the noise level.

D. Dispersive force for nonzero water layer

In the evaluation of the force it will be assumed that water forms a continuous film on the gold surface. In general it can be not the case because water can wet metal surface incompletely due to presence of hydrocarbons and other chemicals on the surface. In the case of incomplete wetting one can use the approach of effective dielectric functions,³² which reduces the problem to a continuous layer with an effective dielectric function. If ϵ_1 is the dielectric function of water in its homogeneous form, then the effective dielectric function $\tilde{\epsilon}_1$ of the material containing a volume fraction of voids f can be found from the equation

$$\frac{\tilde{\epsilon}_1 - \epsilon_H}{\tilde{\epsilon}_1 + 2\epsilon_H} = f \frac{1 - \epsilon_H}{1 + 2\epsilon_H} + (1 - f) \frac{\epsilon_1 - \epsilon_H}{\epsilon_1 + 2\epsilon_H}, \quad (17)$$

where ϵ_H is the dielectric function of the “host” material. In the Bruggman approximation it is assumed that the host material coincides with the effective medium, $\epsilon_H = \tilde{\epsilon}_1$, so it treats both void and material phases on an equal basis. At the imaginary frequencies $\tilde{\epsilon}_1$ with 50% of voids ($f=0.5$) is shown in Fig. 4 as the red line.

We can calculate the force between flat surfaces using the Eqs. (6) and (7). Now for the reflection coefficients we have to use Eqs. (13) and (14) taken at imaginary frequencies.

Figure 5 shows the force at small distances between Au surfaces when both of them are covered with a continuous water layer of thickness $h=0, 1, \text{ and } 1.5 \text{ nm}$. Indeed, the force versus distance between Au surfaces increases with the water layer. This is because the external boundaries of the

bodies (water surfaces) are separated by the smaller distance $d-2h$. As one can see the effect of water becomes very significant at separations d below 10 nm, which are not accessible in this study. We presented only the forces between flat surfaces because at these small separations there is no a reliable way to estimate the roughness correction. The method developed in²⁴ can be applied only for $d \gg w + w_{\text{sph}}$; for the system under investigation this condition is $d \gg 2.3 \text{ nm}$. At distances where the theory is not applicable it was demonstrated experimentally⁹ that the roughness correction increases very significantly, although it was proven for much rougher surfaces than those in the present study.

The effect of water layer on the dispersive force for experimentally investigated separations is shown in Fig. 3 by continuous and dashed black curves, where we included also the effect of roughness. As one can see a continuous layer of a thickness of $h=1.5 \text{ nm}$ is already excluded by the experiment on the level of one standard deviation. However, if there is a discontinuous layer of water containing 50% of air, it is still in agreement with the experiment. We can conclude that the effect of water layer on the dispersive force is considerably masked by large error in the separation upon contact d_0 . On the other hand, for the distances $d < 10 \text{ nm}$ the force measurements are rather limited due to strong jump-up-to contact by formation of capillary bridges.¹⁴ In addition for these distances not only water layer but also roughness is a significant factor, which increases the force up to five times with respect to flat surfaces as our former studies⁹ indicated. All this lead to a rather complex situation at $d < 10 \text{ nm}$.

IV. CONCLUSIONS

In conclusion, we investigated the influence of an ultra thin water layer on the dispersive force between Au surfaces. Evaluation of the force in terms of the Lifshitz theory predicts a strong influence of the water layer on the force, especially for small separations $d < 10 \text{ nm}$, where a higher force is obtained because the effective distance between the Au surfaces decreases. Furthermore, the theoretical predictions are compared to the experimental measurements for distances $d \geq 13 \text{ nm}$ (limited due to strong jump-up-to contact by formation of capillary bridges). It is shown that although the water layer increases the force, it falls within the error margins of the measured force. The errors are shown to arise mainly from the experimental uncertainty in determining the separation upon contact due to nanoscale surface roughness.

Notably at short separations (comparable to the total sphere-plate rms roughness $w_{\text{sph}} + w$) the influence of surface roughness is also significant. The roughness can also strongly increase the force that complicates the situation to a significant degree. In any case, further experimental work is necessary in combination with smoother surfaces to minimize roughness contributions. Roughness is a rather strong barrier because the measurements we did already are at the limits of realistically possible sphere smoothness. The influence of the water layer will be weaker if it wets incompletely the metal surfaces. It can happen due to presence of hydrocarbons and other chemicals leading to a relatively large contact angles 80° .^{13,14}

ACKNOWLEDGMENT

The research was carried out under Project No. MC3.05242 in the framework of the strategic research pro-

gram of the Materials innovation institute (M2i) [the former Netherlands Institute for Metals Research (NIMR)]. Financial support from the Materials innovation institute M2i is gratefully acknowledged.

- ¹A. Cleland, *Foundations of Nanomechanics* (Springer, New York, 2003); P. Ball, *Nature* (London) **447**, 772 (2007); F. Capasso, J. N. Munday, D. Iannuzzi, and H. B. Chan, *IEEE J. Sel. Top. Quantum Electron.* **13**, 400 (2007).
- ²H. B. Chan, V. A. Aksyuk, R. N. Kleiman, D. J. Bishop, and F. Capasso, *Science* **291**, 1941 (2001); *Phys. Rev. Lett.* **87**, 211801 (2001); R. S. Decca, D. López, E. Fischbach, and D. E. Krause, *ibid.* **91**, 050402 (2003).
- ³F. M. Serry, D. Walliser, and G. J. Maclay, *J. Appl. Phys.* **84**, 2501 (1998); E. Buks and M. L. Roukes, *Phys. Rev. B* **63**, 033402 (2001); Wen-Hui Lin, Ya-Pu Zhao, *Chaos, Solitons Fractals* **23**, 1777 (2005); J. Bárcenas, L. Reyes, and R. Esquivel-Sirvent, *Appl. Phys. Lett.* **87**, 263106 (2005).
- ⁴E. M. Lifshitz, *Sov. Phys. JETP* **2**, 73 (1956); I. E. Dzyaloshinskii, E. M. Lifshitz, and L. P. Pitaevskii, *Adv. Phys.* **10**, 165 (1961); E. M. Lifshitz and L. P. Pitaevskii, *Statistical Physics, Part 2* (Pergamon, Oxford, 1980).
- ⁵C. Genet, F. Intravaia, A. Lambrecht, and S. Reynaud, *Annales de la Fondation Louis de Broglie* **29**, 311 (2004).
- ⁶A. Lambrecht and S. Reynaud, *Eur. Phys. J. D* **8**, 309 (2000).
- ⁷D. Tabor and R. H. S. Winterton, *Proc. R. Soc. London, Ser. A* **312**, 435 (1969); J. Israelachvili and D. Tabor, *ibid.* **331**, 19 (1972).
- ⁸T. Ederth, *Phys. Rev. A* **62**, 062104 (2000).
- ⁹P. J. van Zwol, G. Palasantzas, and J. Th. M. DeHosson, *Phys. Rev. B* **77**, 075412 (2008).
- ¹⁰R. Onofrio, *New J. Phys.* **8**, 237 (2006); R. L. Jaffe, *Phys. Rev. D* **72**, 021301(R) (2005).
- ¹¹A. Tonck, F. Houze, L. Boyer, J.-L. Loubet, and J.-M. Georges, *J. Phys.: Condens. Matter* **3**, 5195 (1991).
- ¹²G. Palasantzas, P. J. van Zwol, and J. Th. M. DeHosson, *Appl. Phys. Lett.* **93**, 121912 (2008).
- ¹³H.-J. Butt, B. Cappella, and M. Kappl, *Surf. Sci. Rep.* **59**, 1 (2005); J. N. Israelachvili, *Intermolecular and Surface Forces* (Academic, London, 1992).
- ¹⁴P. J. van Zwol, G. Palasantzas, and J. Th. M. DeHosson, *Phys. Rev. E* **78**, 031606 (2008).
- ¹⁵V. B. Svetovoy, P. J. van Zwol, G. Palasantzas, and J. Th. M. DeHosson, *Phys. Rev. B* **77**, 035439 (2008).
- ¹⁶P. J. van Zwol, G. Palasantzas, M. van de Schootbrugge, and J. Th. M. De Hosson, *Appl. Phys. Lett.* **92**, 054101 (2008).
- ¹⁷P. J. van Zwol, G. Palasantzas, M. van de Schootbrugge, J. Th. M. de Hosson, and V. S. J. Craig, *Langmuir* **24**, 7528 (2008).
- ¹⁸see <http://www.veeco.com/>.
- ¹⁹The yield stress for Au is <100 Mpa (the ultimate strength of Au). A 4 N/m cantilever bends 100 nm after contact with the surface (to determine the deflection sensitivity m) exerts a force of 400 nN onto the surface upon contact. The pressure on a local spot of size say 50 nm is about 160 Mpa, which is above the ultimate stress for Au. Therefore, the features will deform and they do not pose a problem for determining d_0 .
- ²⁰*Handbook of Optical Constants of Solids*, edited by E. D. Palik (Academic, New York, 1995).
- ²¹K. A. Milton, *J. Phys. A* **37**, R209 (2004).
- ²²V. B. Svetovoy and M. V. Lokhanin, *Mod. Phys. Lett. A* **15**, 1013 (2000); M. Lisanti, D. Iannuzzi, and F. Capasso, *Proc. Natl. Acad. Sci. U.S.A.* **102**, 11989 (2005).
- ²³D. Iannuzzi, M. Lisanti, and F. Capasso, *Proc. Natl. Acad. Sci. U.S.A.* **101**, 4019 (2004).
- ²⁴Paulo A. Maia Neto, A. Lambrecht, and S. Reynaud, *Phys. Rev. A* **72**, 012115 (2005); *Europhys. Lett.* **69**, 924 (2005); C. Genet, A. Lambrecht, P. Maia Neto, and S. Reynaud, *ibid.* **62**, 484 (2003).
- ²⁵J. Krim and G. Palasantzas, *Int. J. Mod. Phys. B* **9**, 599 (1995); P. Meakin *Phys. Rep.* **235**, 189 (1993).
- ²⁶G. Palasantzas, *Phys. Rev. B* **48**, 14472 (1993); **49**, 5785 (1994).
- ²⁷V. A. Parsegian and G. H. Weiss, *J. Colloid Interface Sci.* **81**, 285 (1981).
- ²⁸C. M. Roth and A. M. Lenhoff, *J. Colloid Interface Sci.* **179**, 637 (1996).
- ²⁹F. Shubitidze and U. Österberg, *Phys. Rev. E* **75**, 046608 (2007).
- ³⁰R. R. Dagastine, D. C. Prieve, and L. R. White, *J. Colloid Interface Sci.* **231**, 351 (2000).
- ³¹D. J. Segelstein, Ph.D. thesis, The complex refractive index of water, (University of Missouri Press, Kansas City, 1981); see also <http://www.lsbu.ac.uk/water/vibrat.html> and <http://omlc.ogi.edu/spectra/water/index.html>.
- ³²D. E. Aspnes, *Thin Solid Films* **89**, 249 (1982).